The Egyptian Journal of Remote Sensing and Space Sciences (2014) 17, 77–85

National Authority for Remote Sensing and Space Sciences

The Egyptian Journal of Remote Sensing and Space Sciences

www.elsevier.com/locate/ejrs
www.sciencedirect.com

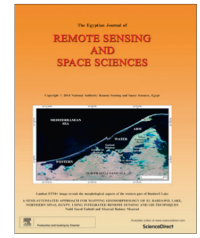

RESEARCH PAPER

Combined use of remote sensing and GIS for degradation risk assessment in some soils of the Northern Nile Delta, Egypt

A.A. El Baroudy [a,*], F.S. Moghanm [b]

[a] *Soil and Water Department, Faculty of Agriculture, Tanta University, Egypt*
[b] *Soil Sciences Department, Faculty of Agriculture, Kafr El Sheikh University, Egypt*

Received 24 October 2013; revised 13 January 2014; accepted 21 January 2014
Available online 19 February 2014

KEYWORDS

Land degradation;
Risk assessment;
Remote sensing;
GIS;
Physiographic mapping

Abstract The present study aimed to assess the potential of Remote Sensing (RS) and Geographic Information System (GIS) to quantify soil degradation risk in some soils of the Northern Nile Delta. Physiographic units were mapped using Landsat ETM+ image (2003) and Digital Elevation Model (DEM). The obtained map showed that the study area comprised two distinct landscapes i.e. fluvial lacustrine and flood plains. The main landforms of the area under consideration are grouped as decantation basins, levees, recent river terraces, overflow basins, man-made terraces, fish ponds and turtle backs. A simple model was designed for assessing risk of land degradation depending on the equations of soil and climatic factors. The study demonstrated that about 48.09% of the study area has undergone very high risk of chemical degradation, whereas 51.91% of the area has undergone low risk of chemical degradation. About 20.12% of the total area was characterized by high risk of physical degradation. The results indicated that the salinity, alkalinity and water logging are the main common degradation hazards.

1. Introduction

Soil degradation is considered one of the most severe global problems worldwide. Annually, about 6 million hectares of agricultural land worldwide becomes unproductive due to various soil degradation processes (Asio et al., 2009). From the agricultural perspective, land degradation is defined as a reduction in soil capacity to produce crops or biomass for humans and livestock. From the ecological perspective, land degradation is seen as damage to the healthy functioning of land-based ecosystems (El Baroudy, 2011). Liberti et al. (2009) reported that soil degradation phenomena occur via a complex interaction between natural (e.g. soil properties and

* Corresponding author. Address: Soil and Water Department, Faculty of Agriculture, Tanta University, 31527 Tanta, Egypt. Tel.: +20 403455584; fax: +20 403455570.
E-mail addresses: drbaroudy@yahoo.com (A.A. El Baroudy), fsaadr@yahoo.ca (F.S. Moghanm).
Peer review under responsibility of National Authority for Remote Sensing and Space Sciences.

Production and hosting by Elsevier

1110-9823
http://dx.doi.org/10.1016/j.ejrs.2014.01.001

climate conditions) and human factors (e.g. over-grazing, over-cultivation and deforestation). The main types of land degradation factors identified in the north Nile Delta include: salinity, sodicity, compaction and water logging as well as water erosion which can be attributed to the Mediterranean Sea level rise (El Baroudy, 2010).

Land degradation can be investigated in different ways, such as direct field observation and remote sensing. In comparison to field methods, the remote sensing technique is more cost-effective and time-efficient in which a huge land area can be monitored using one image. A large number of studies have been carried out using different methods of remote sensing and geographic information system (GIS) to determine land degradation risk. Remotely sensed imagery is appropriate for revealing land that has been affected by degradation to various levels (Gao and Liu, 2008). Furthermore, remotely sensed data are effective in identifying and mapping land degradation risks and modeling soil loss (Chafer, 2008; Geerken and Ilawi, 2004; Lu et al., 2007; Mathieu et al., 2007).

The aims of this study are to: (1) produce the physiographic map of the study area, (2) study the soils of different physiographic units and (3) assess the risk of land degradation depending on remote sensing and GIS techniques and the equations provided by FAO/UNEP (1978, 1979).

2. Materials and methods

2.1. Study area

The study area occupies the northern part of the Nile Delta, Egypt. It is bounded by 30°45′15″ and 30°57′07″ *N* longitude and 30°45′00″ and 31°22′15″ *E* latitude covering an area of 440.63 km^2 (Fig. 1).

The area is characterized by a climate of Mediterranean Sea with hot arid summer and little rain winter. The mean temperature ranges between 15.0 and 30.5 °C in December and August, respectively. The rainfall distribution values occur in the cold season i.e. November–February interval reaching about 167 mm/year. The maximum rainfall values are recorded in January and December. The mean annual evaporation reaches its maximum in August at 7 mm/day. The lowest values are observed in January and December when the temperature is comparatively low, whereas the highest value is recorded in the period between June and September (Climatological Normal for Egypt, 2011).

The study area was formed during the late Pleistocene era which is represented by deposits of the neonile that accumulated during the recessional phases of the river. It was brought to Egypt sometime in the earlier part of this era. Through its history the neonile in this massif has been continually lowering its course at a rate of 1 m/1000 years (Hagag, 1994; Said, 1993). Based on Egyptian Meteorological Authority (1996) and American Soil Taxonomy (USDA, 2010), the soil temperature regime of the studied area was defined as thermic and the soil moisture regime as torric, except for soils having a high water table.

2.2. Digital image processing and map creation

Digital image processing of Landsat 7.0 ETM + satellite images acquired in 2003 was executed using ENVI 4.7© software (ITT, 2009) for classifying the geomorphologic units. Data were

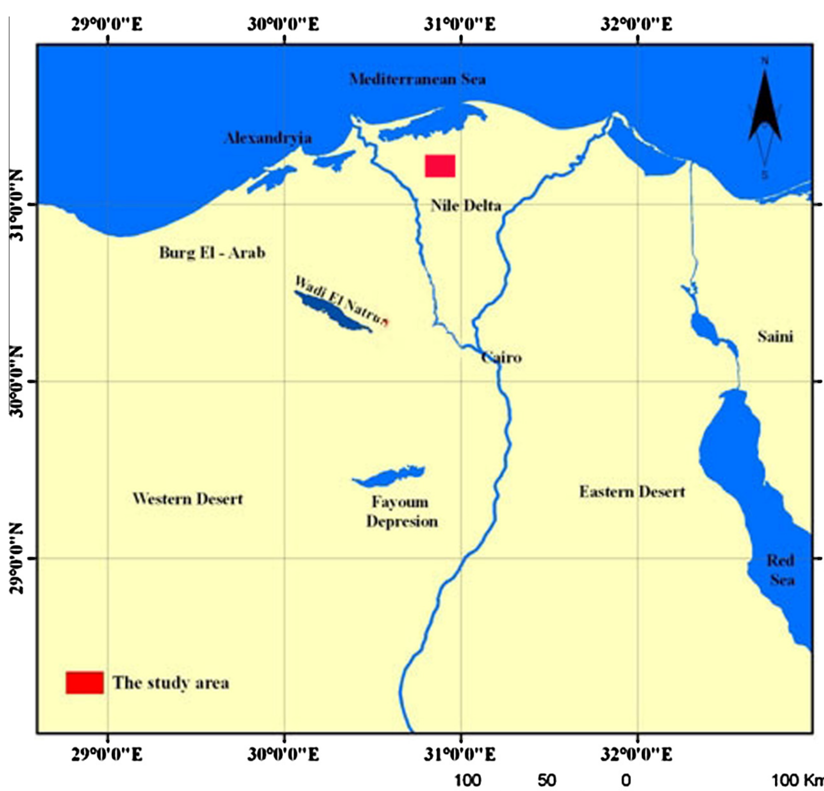

Figure 1 Location of the study area.

calibrated to radiance and manipulated (image stretching, filtering, and histogram matching) according to Lillesand and Kiefer (2007). Atmospheric correction was carried out using FLAASH module in ENVI. The image was georectified to UTM coordinates to be included into the exiting digital image and GIS database. Ground resolution was enhanced using multi-spectral bands (28.50 m) as a low spatial resolution with panchromatic band 8.0 of ETM + satellite image as a high spatial resolution (14.25 m) resulting in multi-spectral data. Fusion methodology was applied according to Ranchin and Wald (2000). The digital elevation model (DEM) of the study area (Fig. 2) was extracted from the Shuttle Radar Topography Mission (SRTM). These

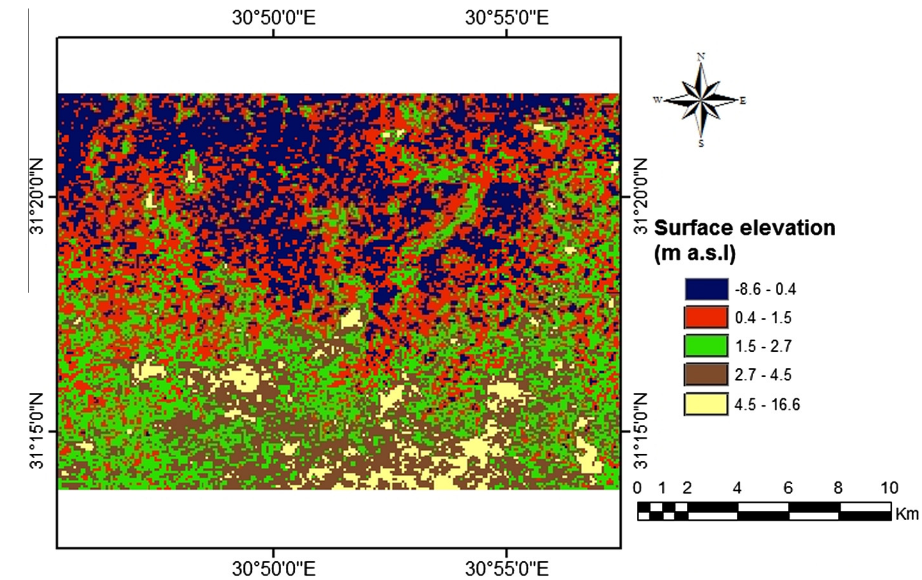

Figure 2 The digital elevation model (DEM) as extracted from SRTM image.

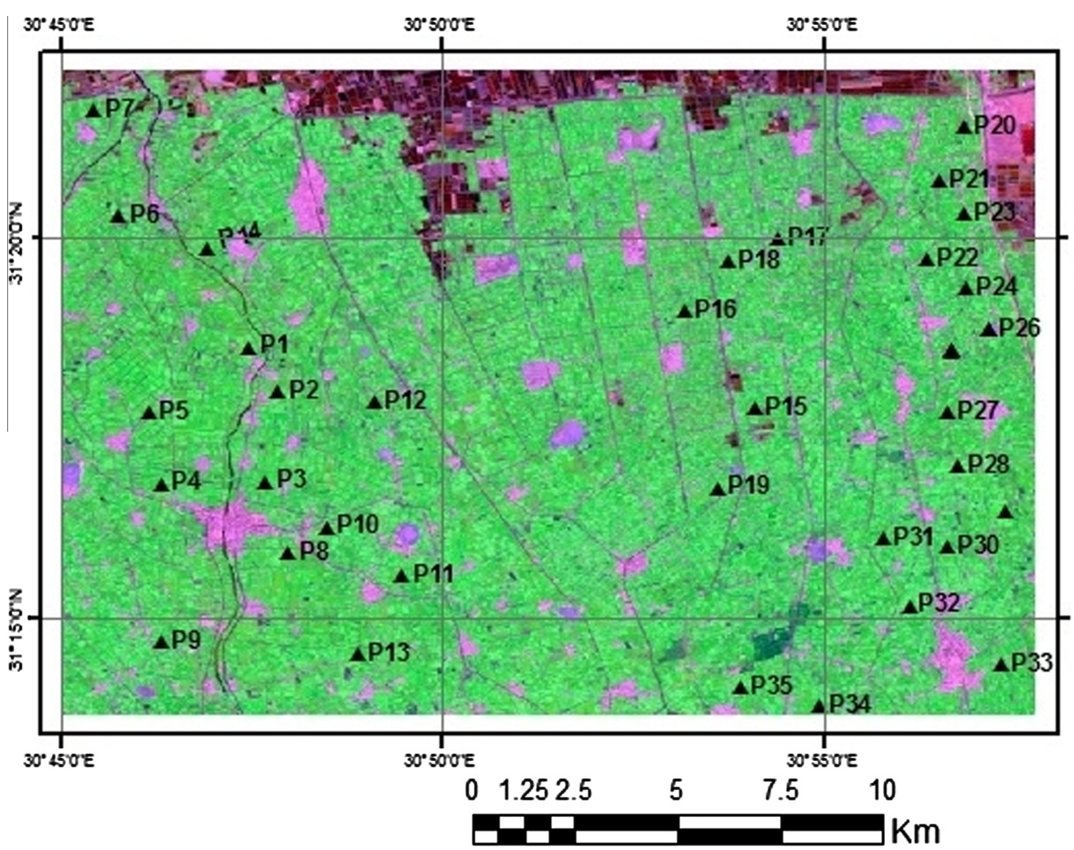

Figure 3 The locations of collected soil profiles.

data can be combined with multispectral images to acquire a better view of the landscape. The Landsat ETM+ image and SRTM data were processed in ENVI 4.7 software to identify different physiographic units according to the approach developed by Dobos et al. (2002). The map legend was designed according to Zinck and Valenzuela (1990). ArcMap 9.2 was used to display and produce geomorphological and spatial distribution maps. Maps have been obtained by matching the physiographic units with field studies and analytical data of salinity, sodicity, bulk density and water table.

2.3. Laboratory analyses and soil taxonomy

Field studies and ground truth data were conducted to identify geomorphologic units and to examine the effectiveness of the satellite imagery interpretation. A total 35 soil profiles (107 soil samples) were taken from three sites (Fig. 3), these sites are representing the whole soil mapping units. A detailed morphological description of the soil profiles was formulated as outlined by FAO (2006). The soil samples were air-dried, grained and passed through 2 mm sieve. The collected fine earths were used for chemical analyses. Electrical conductivity (EC) was determined in saturated soil paste extraction. Exchangeable sodium percentage (ESP) was determined by ammonium acetate (NH_4OAC). Soil bulk density was determined by the core method. Total calcium carbonate was determined volumetrically using Collin's calcimeter method. Particle size distribution of the soil samples was determined according to the pipette method. All laboratory analyses were carried out using the soil survey laboratory methods manual (USDA, 2004). Soils were classified to the sub great group level based on the American Soil Taxonomy (USDA, 2010).

2.4. Land degradation assessment

A simple model for assessing the risk of land degradation was used (Fig. 4) to build a raster GIS based on the equations

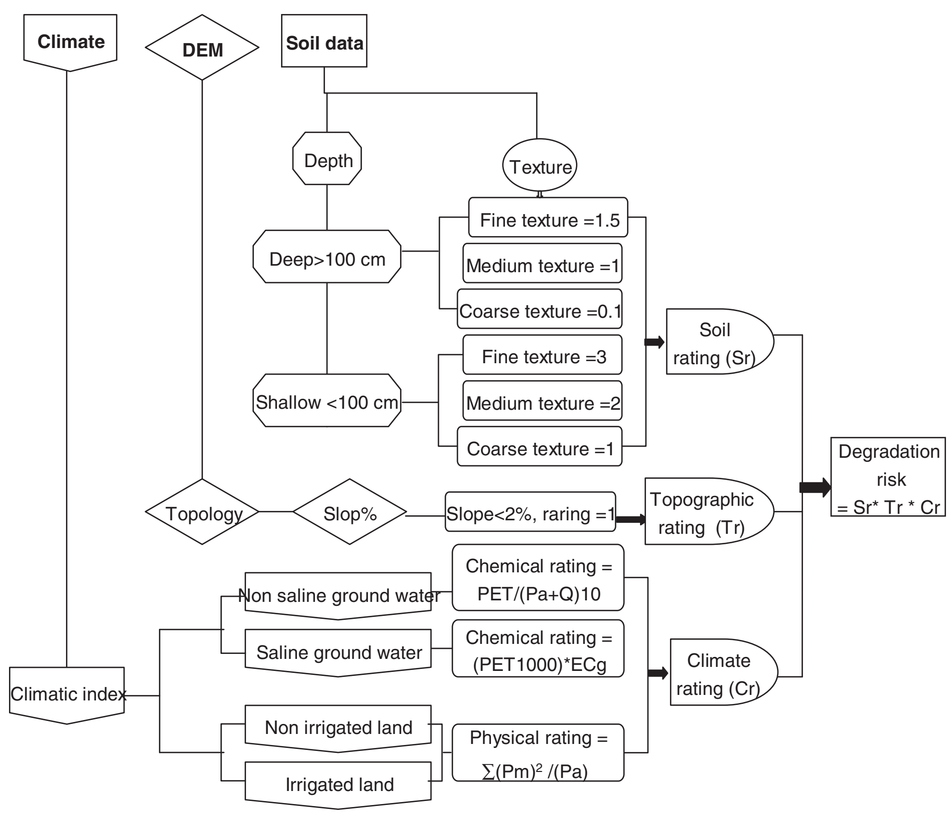

Figure 4 Flowchart of the designed land degradation risk model.

Table 1 Criteria used to determine the degree of the different degradation types.

Critical/hazard type	Indicator	Unit	Hazard class			
			Low	Moderate	High	Very high
Salinization	EC	dS/m	4	4–8	8–16	> 16
Alkalinization	ESP	%	10	10–15	15–30	> 30
Compaction	Bulk density	g/cm^3	1.2	1.2–1.4	1.4–1.6	> 1.6
Water logging	Water table	cm	150	150–100	100–50	< 50

provided by FAO/UNEP (1978, 1979) and the results were evaluated and confirmed with the physiographic units. The criteria used to define and describe the degree and type of salinization, sodication, compaction and water logging are shown in Table 1.

The risk of degradation is governed by several factors i.e. surface slope, soil depth, soil texture, organic matter, soil salinity, ground water salinity, exchangeable sodium percentage, monthly and annually precipitation, potential evapo-transpiration and irrigation water quantity. The influence of these factors can be definite by interpreting their effects on the physical and chemical degradation. The soil texture rating for chemical degradation risk in the deep profiles is 0.1, 1 and 1.5 for coarse, medium and fine texture, respectively. In the case of shallow profiles the used soil rating is 1, 2 and 3 for coarse, medium and fine texture, respectively. The climatic rating of chemical degradation is calculated as follows:

$$CR_c = PET/(P_a + Q)10 \quad (1)$$

Where, CR_c is the climatic rating of chemical degradation risk, PET is the potential evapo-transpiration, P_a is the annual precipitation and Q is the amount of irrigation water used in mm. When using saline ground water, the climatic rating of chemical degradation risk was calculated using the following equation:

$$CR_c = (PET/1000) * EC_{gw} \quad (2)$$

Where EC_{gw} is the ground water salinityThe soil texture rating for physical degradation risk was calculated using Eq. (3):

$$SR_p = S/C \quad (3)$$

Where SR_p is the soil texture rating for physical degradation risk, S is the percentage of silt and C is the percentage of clay.The climatic rating of physical degradation risk was calculated using Eq. (4):

$$CR_p = \sum P_m^2/P_a \quad (4)$$

Where CR_p is the climatic rating of physical degradation risk, P_m is the monthly precipitation in mm and P_a is the annual precipitation in mm.

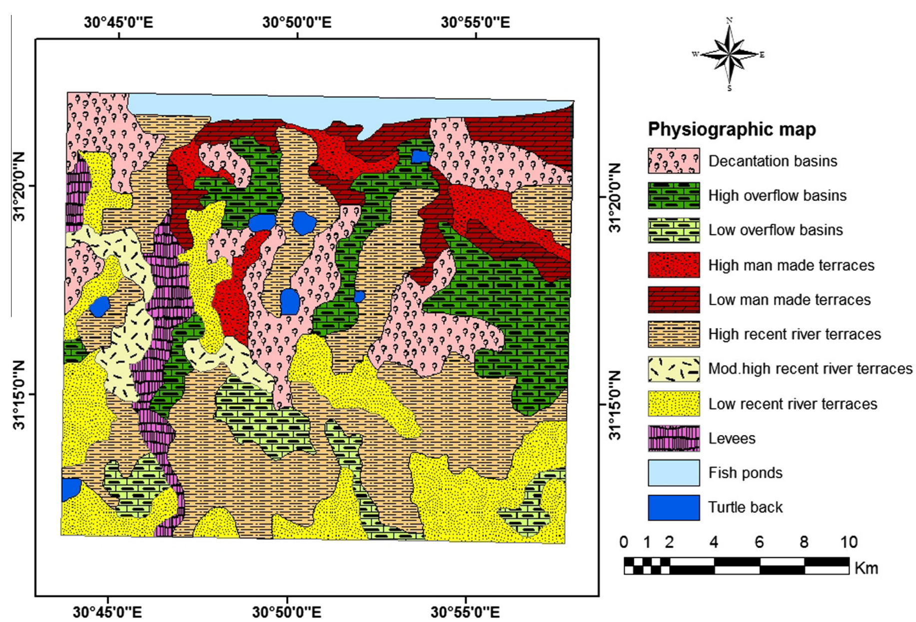

Figure 5 Physiographic map of the studied area.

Table 2 Mean values of some physical and chemical properties of the studied soil profiles.

Mapping units	Soil depth cm	Slope (%)	EC dS/m	ESP	Bulk density (g/cm^3)	$CaCO_3$ (%)	Drainage	Texture class
Decantation basins	110	1.8	4.86	9.7	1.35	1.4	Well	SiCL
High overflow basins	110	2.1	6.63	13.1	1.46	1.3	Poor	SiC
Low overflow basins	100	1.9	1.48	6.07	1.19	3.5	Well	SiC
High man-made terraces	100	1.1	2.29	4.95	1.17	2.6	Well	SiC
Low man-made terraces	100	1.2	15.25	17.3	1.62	2.2	Poor	SiC
High recent river terraces	105	1.4	3.87	7.71	1.32	1.9	Well	C
Mod high recent river terraces	120	1.3	7.24	13.54	1.45	1.8	Well	SiC
Low recent river terraces	120	1.5	2.35	5.02	1.95	1.3	Well	C
Levees	150	0.9	11.65	20.1	1.63	1.7	Poor	SiC

3. Results and discussion

3.1. Physiography and soils

The majority of landscapes in the study area are the fluvio lacustrine plain and flood plain. These landscapes contain different landforms of recent river terraces, decantation basins, overflow basins, levees, man-made terraces turtle backs and fish ponds covering areas of 39.26%, 37.76%, 4.56%, 12.86%, 0.21% and 5.35%, respectively as shown in Fig. 5.

The main units in the study area were overflow basins, decantation basins, levees and terraces. Soil depth, $CaCO_3$ content, texture, salinity, sodicity and drainage condition of the study area range from 80 to 150 cm, 0.4% to 4.2%, silt clay to clay, 1.48 to 15.25 dSm^{-1}, 4.95% to 20.1% and poor to well, respectively (Table 2). Soil profiles were classified into two soil orders. The first was Entisols with sub great groups of *Typic Torrifluvent* and *Vertic Torrifluvent*. The second order was Aridisols with sub great groups *of Typic Haplosalids*, *Aquallic Salorthids*, and *Typic Natrargids*.

3.2. Soil degradation hazard assessment

The attribute data tables for salinity, alkalinity, bulk density and water table were compiled into the digital geomorphologic

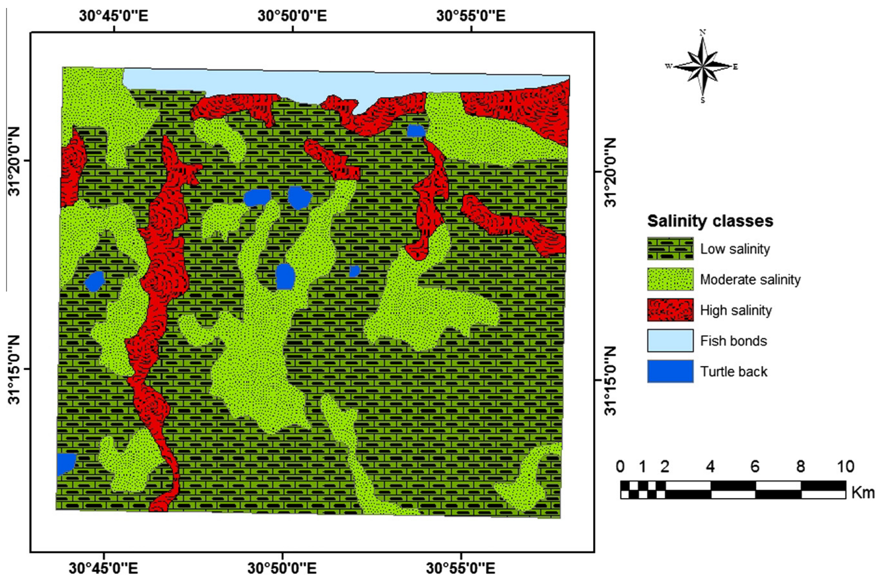

Figure 6 Spatial distribution of soil salinity classes.

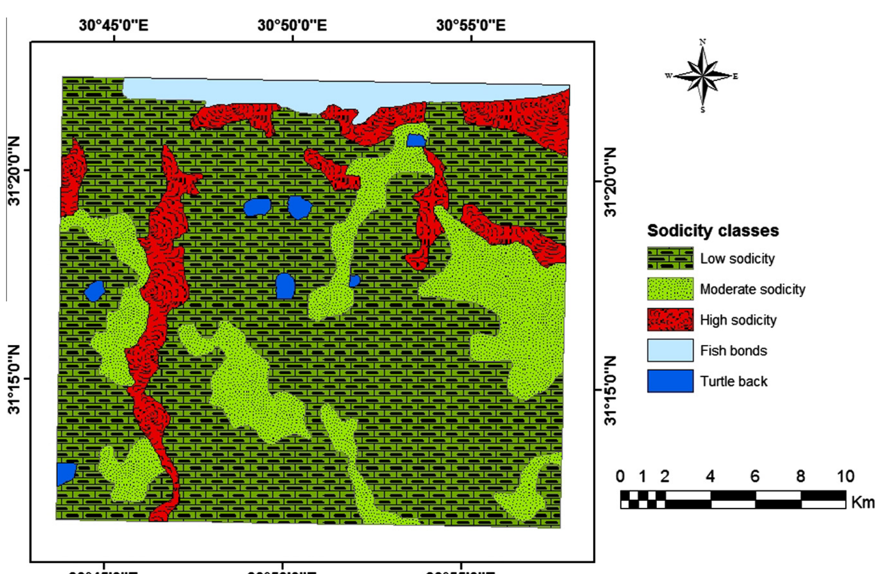

Figure 7 Spatial distribution of soil sodicity classes.

map units in a geographic information system. The incorporated attributes were used to obtain the thematic layers of spatial distribution of the above mentioned characteristics (Figs. 6–9). Salinity, sodicity and water logging are the main degradation hazards in the studied area. They were defined in relation to values of electrical conductivity (EC), exchangeable sodium percentage (ESP) and the depth of water table, respectively. The very high hazard of compaction was present in 12.32% of the total area as a result of human activities, inadequate soil management, using heavy machinery and human intervention in natural drainage systems. The soils affected by a high hazard of salinity, sodicity, compaction and water logging represented 13.68%, 12.92%, 31.11% and 23.72% of the total area, respectively. Moderate hazard of salinity, sodicity, compaction and water logging was found in different landforms representing 48.01%, 31.11%, 27.42% and 67.06% of the total area, respectively.

Regarding human activities, the main types of land degradation in the investigated areas were salinization, alkalinization, soil compaction and water logging. Human induced salinization and alkalinization can be the result of the two causes, firstly, poor management of irrigation schemes. A high salt content of irrigation water or too little attention given to the drainage of irrigated fields may lead to rapid salinization, this pattern of salt accumulation mainly occurs under arid and semi-arid conditions. A second type occurs where human activities lead to increased evapo-transpiration of soil moisture

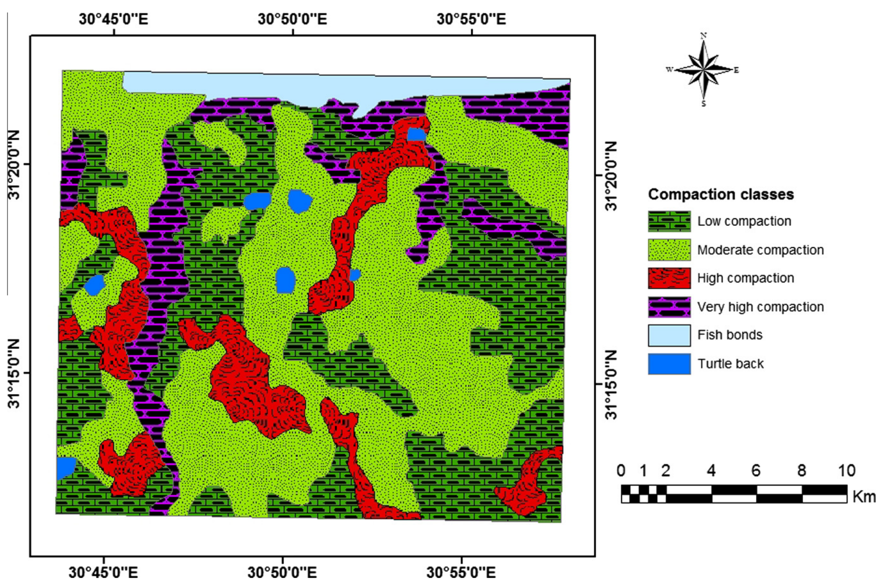

Figure 8 Spatial distribution of soil compaction.

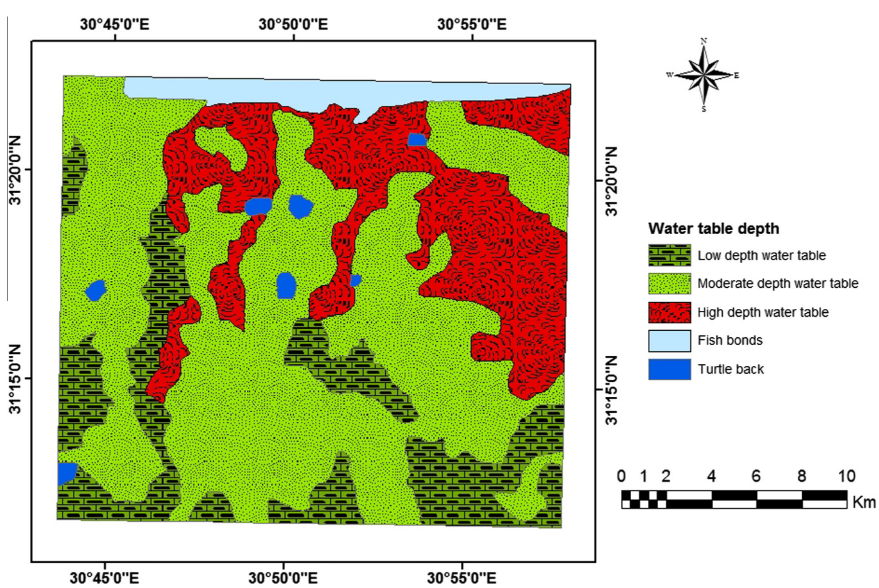

Figure 9 Spatial distribution of water table depth.

Table 3 The computed chemical and physical degradation risks in the studied area.

Mapping units	Chemical degradation					Physical degradation				
	SR	TR	CR	Risk	Class	SR	TR	CR	Risk	Class
Decantation basins	1	1	0.02	0.02	1	0.66	1	1.69	1.12	2
High overflow basins	1	1	0.02	0.02	1	0.79	1	1.69	1.34	2
Low overflow basins	1	1	21.6	21.6	4	0.80	1	1.69	1.35	3
High man-made terraces	1	1	0.02	0.02	1	0.57	1	1.69	0.96	1
Low man-made terraces	1	1	21.46	21.46	4	0.98	1	1.69	1.66	2
High recent river terraces	1.5	1	0.02	0.03	1	0.64	1	1.69	1.08	2
Mod high recent river terraces	1	1	7.46	7.46	4	0.91	1	1.69	1.54	1
Low recent river terraces	1.5	1	9.25	13.88	4	0.75	1	1.69	1.27	3
Levees	1	1	10.5	10.5	4	0.68	1	1.69	1.15	3

SR, soil rating; TR, topographic rating; CR, climatic rating; Risk = SR*TR*CR; risk < 2 (class = 1 low), risk = 2–4 (class = 2 moderate), risk = 4–6 (class = 3 high), risk > 6 (class = 4 very high).

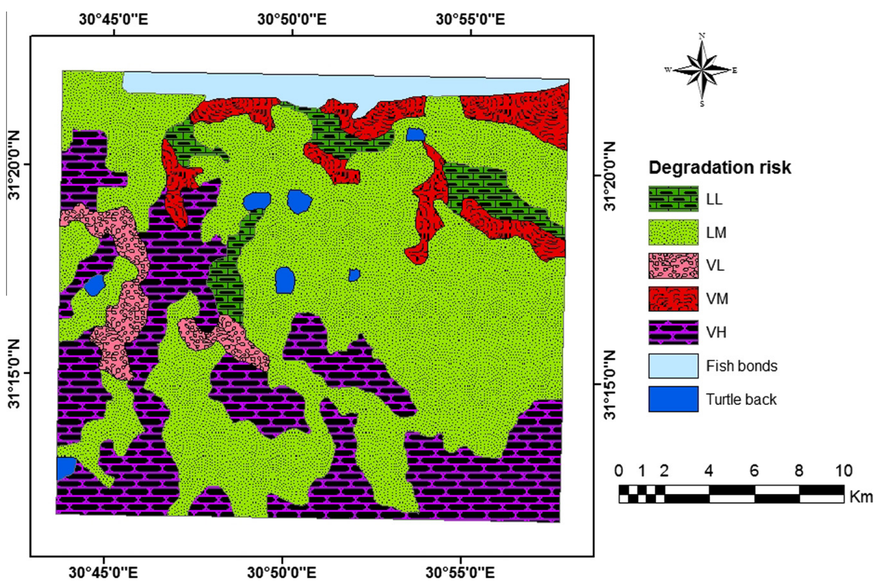

Figure 10 Degradation risk map of the studied area. The first letter = chemical degradation risk and the second letter = physical degradation risk; L, low; M, moderate; H, High; V, very high risk.

in areas of high salt-containing parent materials or with saline ground water.

3.3. Soil degradation risk assessment

Soil degradation risk is considered as the diminution of current or potential productivity resulting from the action of climate, soil and topography without the intervention of human effect. Analysis of DEM data indicated that the slope gradient in the study area ranged between 0.9% and 2.1%, which has a slight effect on natural vulnerability. Thus the topographic effect on natural vulnerability was considered as 1.0 in different landforms.

The degradation risk of the study area is represented in Table 3 and Fig. 10. The risk of chemical degradation was classified as very high in all including the levees, low recent river terraces, low overflow basins, moderately high recent river terraces and low man-made terraces. These soils covered an area of 211.9 km^2 representing 48.09% of the study area. About 228.73 km^2 representing 51.91% of the total area were characterized by low risk of chemical degradation. The risk of physical degradation ranged between low and high classes throughout the whole study area. The areas threatened by high risk values were located in the levees, low recent river terraces and low overflow basins covering an area of 88.66 km^2 (20.12% of the total area).

4. Conclusion

The study has demonstrated that the severity and susceptibility of land degradation can be studied by harnessing technologies such as remote sensing and GIS. The research indicated that about 48.09% and 20.12% of the total area were characterized by a very high and high risk of chemical and physical degradation, respectively. The studied soils are threatened by a low to high degree of water logging, compaction, salinity and alkalinity. The high values of hazard can be attributed to the excessive irrigation practices, improper use of heavy machinery and absence of conservation measures. The human impact on land degradation processes could be reflected in view of degradation risk and the actual hazard. Where, the high risk and low actual degradation indicate the positive human impact and vice versa. The present scenario of land degradation in the study area is very alarming and needs proper land use planning and management.

Acknowledgements

The authors are greatly indebted to Prof. S.M. Shams, Prof. Abo Wally M.E. Department of Soil, Faculty of Agriculture, Kafr Elsheikh University, and Prof. H. Ismail Department of Soil and Water, Faculty of Agriculture, Alexandria University, for their valuable and critical comments and also for their help in revising this manuscript.

References

Asio, V.B., Jahn, R., Perez, F.O., Navarrete, I.A., Abit, S.M., 2009. A review of soil degradation in the Philippines. Ann. Trop. Res. 31 (2), 69–94.

Chafer, C., 2008. A comparison of fire severity measures: an Australian example and implications for predicting major areas of soil erosion. Catena 74, 235–245.

Climatological Normal for Egypt., 2011. The Normal for Kafr El-Sheikh Governorate from 1960 to 2011. Ministry of Civil Aviation, Meteorological Authority, Cairo, Egypt.

Dobos, E., Norman, B., Bruee, W., Luca, M., Chris, J., Erika, M., 2002. The Use of DEM and Satellite Images for Regional Scale Soil Database. 17th World Congress of Soil Science (WCSS), Bangkok, Thailand (14–21 August 2002).

Egyptian Meteorological Authority., 1996. Climatic Atlas of Egypt. Published. Arab Republic of Egypt. Ministry of Transport.

El Baroudy, A.A., 2010. Geomatics based soil mapping and degradation risk assessment of some soils east Nile Delta, Egypt. Pol. J. Environ. Stud. 19 (6), 1123–1131.

El Baroudy, A.A., 2011. Monitoring land degradation using remote sensing and GIS techniques in an area of the middle Nile Delta, Egypt. Catena 87 (2), 201–208.

FAO/UNEP., 1978. Methodology for Assessing Soil Degradation. Rome, 2527 Italy.

FAO/UNEP, 1979. A Provisional Methodology for Soil Degradation Assessment. FAO, Rome, Italy (M-57 ISBN 92-5-100869-8).

FAO, 2006. Guidelines for Soil Description, fourth ed. FAO, Rome, Italy.

Gao, J., Liu, Y., 2008. Mapping of land degradation from space: a comparative study of Landsat ETM+ and ASTER data. Int. J. Remote Sens. 29 (14), 4029–4043.

Geerken, R., Ilawi, M., 2004. Assessment of rangeland degradation and development of a strategy for rehabilitation. Remote Sens. Environ. 90 (4), 490–504.

Hagag, A., 1994. Soil Classification of Northern Coast of Delta (Ph.D. thesis). Mansoura University, Egypt.

ITT., 2009. ITT Corporation ENVI 4.7 Software, 1133 Westchester Avenue, White Plains, NY 10604, USA.

Liberti, M., Simoniello, T., Carone, M.T., Coppola, R., Emilio, M.D., Macchiato, M., 2009. Mapping badland areas using LANDSAT TM/ETM satellite imagery and morphological data. Geomorphology 106, 333–343.

Lillesand, T.M., Kiefer, R.W., 2007. Remote Sensing and Image Interpretation, fifth ed. John Wiley, New York, p. 820.

Lu, D., Batistella, M., Mausel, P., Moran, E., 2007. Mapping and monitoring land degradation risks in the Western Brazilian Amazon using multitemporal Landsat TM/ETM+ images. Land Degrad. Dev. 18, 41–54.

Mathieu, R., Cervelle, B., Remy, D., Pouget, M., 2007. Field-based and spectral indicators for soil erosion mapping in semi-arid Mediterranean environments (Coastal Cordillera of central Chile). Earth Surf. Proc. Land. 32, 13–31.

Ranchin, T., Wald, L., 2000. Fusion of high spatial and spectral resolution images: the ARSIS concept and its implementation. Photogramm. Eng. Remote Sens. 66 (1), 49–61.

Said, R., 1993. The River Nile Geology and Hydrology and Utilization. Pergman Press, Oxford, Britain, p. 320.

USDA., 2004. Soil Survey Laboratory Methods Manual Soil Survey Investigation Report No. 42 Version 4.0.

USDA, 2010. Keys to Soil Taxonomy, 11th ed. United State Department of Agriculture, Natural Resources Conservation Service (NRCS).

Zinck, J.A., Valenzuela, C.R., 1990. Soil geographic database: structure and application examples. ITC-Journal 3, 270.